# Ambient IoT: Transmit Power Minimization for NOMA-Enabled BackCom

Diluka Galappaththige[†], Fatemeh Rezaei[†], Chintha Tellambura[†], and Amine Maaref[‡]
[†]Department of Electrical and Computer Engineering, University of Alberta, Edmonton, AB, T6G 1H9, Canada
[‡]Huawei Canada, 303 Terry Fox Drive, Suite 400, Ottawa, Ontario K2K 3J1
Email: {diluka.lg, rezaeidi, ct4}@ualberta.ca, amine.maaref@huawei.com

***Abstract*—Ambient internet-of-things networks are just emerging to support sixth-generation wireless goals. We thus investigate a symbiotic radio (SR) system for a single-user primary network and a backscatter communication network that supports non-orthogonal multiple access. The primary base station (BS) concurrently supports the primary user and multiple tags, which modulate and reflect their data using the primary BS signal. The user decodes its data and the tags' data using the successive interference cancellation technique. We propose a novel optimization framework to accommodate the requirements of both the primary user and the tags while also improving SR network performance. By constructing the beamforming vectors to support both primary and backscatter networks, we develop a BS transmit power minimization problem. The problem formulation ensures the various quality-of-service demands of the user and the tags and the tag energy harvesting requirements. Because of the non-convexity of the problem, we employ semi-definite relaxation techniques to obtain a sub-optimal solution. We evaluate the computational complexity of the proposed algorithm. Finally, we present extensive numerical results and simulations that establish the validity and performance gains of the proposed optimization scheme without modifying the fundamental passive tag architecture.**

## I. Introduction

Ambient power-enabled Internet-of-Things (IoT) has recently emerged as a hot research topic, and the 3rd generation partnership project (3GPP) has launched a new study item [1]. Reducing the size, complexity, and power consumption of IoT devices can enable the deployment of tens or even hundreds of billions of IoT devices for a variety of applications such as logistics, inventory management, warehousing, manufacturing, and many others [2], [3].

IoT devices, on the other hand, are powered by batteries that must be replaced or recharged manually. This results in significant maintenance costs, serious environmental concerns, and even potential safety hazards for specific use cases (e.g., wireless sensors for power and petroleum industries). Because energy harvesting (EH) output power typically ranges from $1\,\mu\mathrm{W}$ to a few hundred $\mu\mathrm{W}$, existing cellular devices with $10\,\mathrm{mW}$ peak power consumption may not perform well with EH [1]. As a remedy, batteryless devices with no energy storage capabilities (i.e., passive) or devices with limited energy storage (i.e., semi-passive) will meet massive connectivity requirements. Ambient backscatter communication (AmBC) systems, in particular, have the potential to enable future ambient IoT networks and applications [2], [4].

These systems leverage ambient radio frequency (RF) sources, such as cellular base stations (BSs), TV towers, and Wi-Fi access points. The tags use those signals to harvest energy and backscatter data [2], [3], [5]. Since they do not generate RF signals, they are inexpensive and have extremely low energy requirements (a few $\mathrm{nW}$–$\mu\mathrm{W}$) [2], [5]. Spectrum utilization improves as AmBC systems eschew new frequency spectrum allocations. However, legacy signals can directly interfere, limiting the AmBC performance. Sophisticated methods are thus required to deal with direct link interference [6].

Nonetheless, a common receiver can decode both AmBC and primary legacy systems. Instead of treating the legacy signal as interference, it leads to symbiotic radio (SR), which can support both primary and tag transmissions [4]. The primary receiver decodes the data from the primary transmitter and the tag [4], [7]. In particular, when decoding tag signals, it first decodes the primary signal and then subtracts it from the received signal. Hence, maintaining both primary and tag performance necessitates multi-objective optimization techniques and efficient resource allocation [8].

The tags require a multiple access scheme. Hence, non-orthogonal multiple access (NOMA) can accommodate multiple tag transmissions while increasing spectrum efficiency and throughput [9]. In contrast to orthogonal multiple access (OMA), NOMA allows multiple users to concurrently communicate on each orthogonal channel. Power-domain NOMA separates multiple user signals based on channel gain differentials and detects individual user signals using successive interference cancellation (SIC) [10]. **The incorporation of NOMA into the SR configuration increases the number of connected tags and may result in spectral and energy efficiency gains for large-scale ambient IoT networks. As a result, NOMA-enabled SR networks are an extremely important research topic.**

### A. Problem Statement and Contributions

Ambient IoT can be realized by combining NOMA and an SR network (Fig. 1), increasing spectral efficiency and device connectivity. The tags in this setup use the primary BS signal to communicate with a primary user via NOMA. To do this, the BS must support the primary user and tag transmissions. Specifically, the BS beamforming design should simultaneously satisfy the minimum quality-of-service (QoS) of the primary user and the tags, i.e., minimum rate requirements, as well as the EH constraints at the tags. Furthermore, reducing BS power consumption while maintaining minimum QoS is critical to supporting massive connectivity. Thus, we will investigate the system model in Fig. 1 to fill a significant gap in the ambient IoT literature, i.e., *power consumption*

*and massive connectivity*. Specifically, integrating NOMA and SR, and minimizing BS power consumption while maintaining minimum QoS, are two potential solutions to support massive connectivity as a key requirement of ambient IoT. However, how much benefit do these two approaches provide? To date, no work has answered this question.

The primary goal of this paper is to bridge that gap by further researching SR networks to enable ambient IoT. In particular, we consider a NOMA-assisted SR network with multiple tags coexisting with a primary user (Fig. 1). Since the tags are passive devices, they harvest energy from the primary BS signal and transmit their data to the user via backscattering. We use NOMA to effectively mitigate interference from one tag to another as different tag signals collide.

Previous studies only consider a single-antenna BS [8], [11]. In contrast, we treat a BS with an array of antennas, which gives the BS spatial degrees of freedom. We can use it to improve performance. Thus, we design transmit beamforming to minimize BS transmit power while maintaining the primary user and tags rate constraints, and tags' EH constraints. Because of the non-convex constraints, this transmit power minimization (TPMin) problem is non-convex. We use the semi-definite relaxation (SDR) technique and propose an algorithm to find a sub-optimal solution. We show that incorporating NOMA into an SR network along with the proposed resource allocation algorithm results in significant gains. Specifically, optimal beamforming designs at the BS increase the number of connected tags while satisfying the QoS of the primary user and the tags, and the tags' EH constraints. Finally, we present extensive numerical examples to evaluate the performance of the NOMA-enabled SR setup using the proposed solutions.

Next, we present the related works to provide the context and background for our work.

### B. Previous Contributions on NOMA-Enabled SR Systems

NOMA-enabled SR systems have received little attention due to the limited processing power and resources at passive tags, except for [8], [11]. Nevertheless, massive connectivity for backscatter devices is necessary for developing future ambient IoT networks, which is where NOMA-enabled backscatter communication (BackCom)/SR is essential.

Reference [8] investigates a NOMA-assisted dynamic time-division-multiple-access (TDMA) scheme for an SR network. This scheme categorizes backscatter devices into several clusters. Only one cluster transmits during each time slot, and the tags in it use NOMA access. Then, under the primary user's rate constraint and EH constraints at the tags, the minimum throughput among all tags is maximized by jointly optimizing tag reflection coefficients, the BS power allocation in different time slots, and the time allocation. The NOMA+TDMA scheme is further investigated in [11] for a full-duplex SR network, where a BS transmits downlink orthogonal frequency division multiplexing signals to a primary user and simultaneously receives signals from multiple tags. The authors then maximize the minimum throughput among all tags by optimizing the BS sub-carrier power allocation, time allocation, and tag reflection coefficients, subject to the primary user throughput requirement and the EH constraints at the tags.

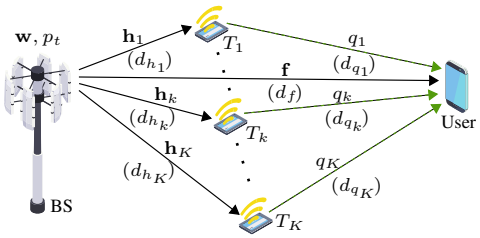


**Fig. 1:** A NOMA-enabled BackCom system setup.

These research works consider single-antenna BS and perform the resource allocation under perfect CSI. Besides, the effort is to ensure fairness between the tags while meeting the QoS of the primary user. Additionally, [8] and [11] both consider optimizing the tag's reflection coefficient, which may not be feasible with passive tags because of the limited power availability.

*Notation*: Lowercase bold and uppercase bold denote vectors and matrices. $\mathbf{A}^{\mathrm{H}}$ and $\mathrm{Tr}(\mathbf{A})$ denote Hermitian transpose and trace of $\mathbf{A}$. $\mathbb{E}\{x\}$ is the mean of $x$. Further, $\mathcal{CN}(\boldsymbol{\mu}, \mathbf{R})$ is a complex Gaussian vector with mean $\boldsymbol{\mu}$ and co-variance $\mathbf{R}$. Finally, $\mathcal{K} \triangleq \{1, \ldots, K\}$, $\mathcal{K}'_k \triangleq \{k+1, \ldots, K\}$, and $\mathcal{K}_0 \triangleq \{0, 1, \ldots, K\}$.

## II. System Model and Preliminaries

### A. System and Channel Models

In Fig. 1, we consider an SR network having an $M \geq 1$ antenna BS, as the primary transmitter, communicating with a single-antenna primary user, and single-antenna $K$ tags, denoted by $T_k, k \in \mathcal{K}$, which leverage the primary signal to transmit their data to the user. The tags are passive devices, i.e., they do not have any RF source, and hence they harvest energy from the primary signal and perform backscatter modulation for data transmission. Therefore, the BS beamforms the transmit signal to the user while powering the tags to send their data to the user. We use the power-domain NOMA technique to transmit data from the tags [9], [11].

For the system, we consider block flat-fading channel models. Thus, $\mathbf{f} \in \mathbb{C}^{M\times 1}$ denotes the direct channel from the BS to the user during each fading block. The backscatter channel through $T_k$ is $\mathbf{g}_k = \mathbf{h}_k q_k, k \in \mathcal{K}$, which is the product of the forward channel from the BS to $T_k$ ($\mathbf{h}_k \in \mathbb{C}^{M\times 1}$) and the backward channel from $T_k$ to the user ($q_k \in \mathbb{C}$). All channels are assumed to be independent quasi-static Rayleigh fading that remains constant throughout the coherence interval. A unified representation of all channels is given as $\mathbf{a} \sim \mathcal{CN}(\mathbf{0}, \zeta_{\mathbf{a}}\mathbf{I}_M)$, where $\mathbf{a} \in \{\mathbf{f}, \mathbf{h}_k, q_k\}$ and $\zeta_{\mathbf{a}}$ is the large-scale path-loss and shadowing.

For the proposed SR system (Fig. 1), the CSI can be acquired through pilot-based channel estimation during uplink transmission [12].

### B. Tags' Data Transmission and EH

As previously stated, tags are passive devices and rely entirely on EH. In particular, $T_k$ harvests energy from the power

received at its antenna, $p_k^a$. The tags use the harvested power for operating their essential circuits and perform backscatter modulation for data transmission. The reflection coefficient at $T_k$, $\alpha_k$, depends on the tag's modulation scheme [2], [3]. Here, we assume a common reflection coefficient for all tags, i.e., $\alpha_k = \alpha\,(k \in \mathcal{K})$. Then, $\alpha p_k^a$ of the received RF power is backscattered while the remainder, $p_k^{in} = (1-\alpha)p_k^a$, propagates to the EH circuit, where $\alpha$ satisfies $0 < \alpha < 1$.

Using a rectifier, the EH circuit converts RF power, $p_k^{in}$, to direct current (DC) power. In general, the EH model determines the amount of harvested power at the tag. For the sake of simplicity, we assume the linear EH model at the tag. The harvested DC power at $T_k$, $p_k^h$, is given as $p_k^h = \eta_b p_k^{in}$, where $\eta_b$ $(0 < \eta_b \leq 1)$ is the energy conversion efficiency, and it is assumed to be a constant independent of the incident RF power, $p_k^{in}$. Despite the fact that practical EH circuits have non-linear operating characteristics and an activation threshold, the linear model can be precise in certain operating regions. However, our solution can be applied to non-linear EH models as well. We omit the details for brevity.

Because the tag is passive, its harvested power, $p_h$, must exceed a minimum threshold in order for it to function, i.e., $p_h \geq p_b$, $p_b$ denotes the minimum required power at the tag, e.g., about $-20\,\mathrm{dBm}$ for commercial passive tags [8].

### C. Transmission Model

The BS sends a signal $s(n)$ with the transmit power of $p_t$ to the user, where $\mathbb{E}\{|s(n)|^2\} = 1$. The BS transmitted signal at the $n$-th time slot is thus given as $x(n) = \sqrt{p_t}s(n)$. The tags use $x(n)$ for EH, modulating their binary signals, $c_i(n)$ $(\mathbb{E}\{|c_i(n)|^2\} = 1$ for $i \in \mathcal{K})$, and then transmitting them to the user. The user receives the BS signal and the tags' signals. The received signal at the user is given as

$$y(n) = \mathbf{f}^{\mathrm{H}}\mathbf{w}x(n) + \sqrt{\alpha}\sum\nolimits_{i\in\mathcal{K}} \mathbf{g}_i^{\mathrm{H}}\mathbf{w}x(n)c_i(n) + z(n), \quad (1)$$

where the first and second terms in $y(n)$ are the direct-link signal and the backscattered-link signal, respectively. In (1), $\mathbf{w} \in \mathbb{C}^{M\times 1}$ $(\|\mathbf{w}\|^2 = 1)$ is the BS beamforming vector and $z(n) \sim \mathcal{CN}(0, \sigma^2)$ is the additive white Gaussian noise (AWGN) at the user having 0 mean and $\sigma^2$ variance. Here, we assume that the primary signal $s(n)$ and the tag signals $c_i(n), i \in \mathcal{K}$, are standard circular symmetric complex Gaussian distributed $\mathcal{CN}(0, 1)$ [4].

Without compromising generality, we assume that tags with lower indexes have higher effective channel gains than tags with higher indexes to implement power domain NOMA, i.e., $|\mathbf{g}_1^{\mathrm{H}}\mathbf{w}|^2 \geq \ldots \geq |\mathbf{g}_K^{\mathrm{H}}\mathbf{w}|^2$. Thereby, the user adopts SIC to decode the tags' signals. In particular, because the direct-link signal is usually stronger than the backscatter-link signal, the user decodes its own signal first, treating tag signals as interference [4]. The user then subtracts the decoded signal, $s(n)$, from the received signal, $y(n)$, and decodes each tag signal using SIC decoding. The post-processed signal for decoding $T_k$'s data at the user is given as

$$y_k(n) = \underbrace{\sqrt{\alpha p_t}\mathbf{g}_k^{\mathrm{H}}\mathbf{w}s(n)c_k(n)}_{\text{Desired signal}} + \underbrace{\sqrt{\alpha p_t}\sum\nolimits_{i\in\mathcal{K}'_k} \mathbf{g}_i^{\mathrm{H}}\mathbf{w}s(n)c_i(n)}_{\text{Tag interference after SIC}} + \underbrace{z(n)}_{\text{AWGN}}. \quad (2)$$

### D. Achievable Rate

Herein, we derive the rates of the user and the tags. From the received signal (1), the rate of the user is computed as $\mathcal{R}_0 = \log_2(1+\gamma_0)$, where

$$\gamma_0 = \frac{p_t|\mathbf{f}^{\mathrm{H}}\mathbf{w}|^2}{\alpha p_t \sum_{i\in\mathcal{K}}|\mathbf{g}_i^{\mathrm{H}}\mathbf{w}|^2 + \sigma^2}. \quad (3)$$

Next, the user performs SIC to decode the tag signals. From the post-processed signal (2), the rate of $T_k$ is given as

$$\mathcal{R}_k = \mathbb{E}_s\left\{\log_2(1+\gamma_k^b)\right\}, \quad (4)$$

where $\gamma_k^b$ is the signal-to-interference-plus-noise ratio (SINR) of $T_k$ at the user, which is given as

$$\gamma_k^b = \frac{\alpha p_t|\mathbf{g}_k^{\mathrm{H}}\mathbf{w}|^2|s(n)|^2}{p_t\alpha\sum_{i\in\mathcal{K}'_k}|\mathbf{g}_i^{\mathrm{H}}\mathbf{w}|^2|s(n)|^2 + \sigma^2}. \quad (5)$$

By taking the average over $s(n)$ in (4), the rate of $T_k$ is computed as[1]

$$\mathcal{R}_k = \log_2(e)\left(-e^{\frac{1}{a_k+b_k}}\mathrm{E}_i\left(\frac{-1}{a_k+b_k}\right) + e^{\frac{1}{b_k}}\mathrm{E}_i\left(\frac{-1}{b_k}\right)\right), \quad (6)$$

where

$$a_k \triangleq \frac{\alpha p_t}{\sigma^2}|\mathbf{g}_k^{\mathrm{H}}\mathbf{w}|^2, \quad \text{and} \quad b_k \triangleq \frac{p_t\alpha}{\sigma^2}\sum\nolimits_{i\in\mathcal{K}'_k}|\mathbf{g}_i^{\mathrm{H}}\mathbf{w}|^2. \quad (7)$$

Further, $\mathrm{E}_i(x) = \int_{-\infty}^{x} u^{-1}e^u du$ is the exponential integral function. Note that, $-e^{\frac{1}{x}}\mathrm{E}_i(-1/x)$ is monotonically increasing and concave function of $x$ [4].

According to Section II-B, the tags must harvest enough power to maintain their circuit operation. Hence, the following constraint must be satisfied for $T_k$ to function: $\eta_b(1-\alpha)p_k^a \geq p_b$, where $p_k^a = p_t|\mathbf{h}_k^{\mathrm{H}}\mathbf{w}|^2$ is the received power at $T_k$ antenna.

## III. Optimization Problem Formulation

In this section, we optimize the performance of the NOMA-enabled SR network (Fig. 1). Specifically, we minimize the BS transmit power, $p_t$, by optimizing the BS transmit beamforming vector, $\mathbf{w}$, while meeting minimum rate requirements for all devices and tags' EH requirements. The problem addresses a vital concern for enabling ambient IoT by increasing the number of connected tags for the realization of large-scale ambient IoT networks. Additionally, power consumption is a critical metric for green system design. High BS power consumption limits the number of connected devices in a cellular network. Hence, reducing power consumption while

[1]For $s(n) \sim \mathcal{CN}(0,1)$, the square envelope of $s(n)$ follows the exponential distribution.

maintaining a minimum QoS for applications is critical, given the rapid increase in the number of connected devices toward establishing massive machine-type communication (mMTC). To that end, our SR network is a promising mMTC candidate.

Our formulation considers tags with a fixed reflection coefficient. A fixed reflection coefficient will greatly simplify the implementation of passive tags [13]. On the other hand, if the reflection coefficient is included in the optimization process, the tags must be able to adjust it dynamically. The resulting tag architecture may raise the cost and power consumption of each tag, which is incompatible with the goals of ambient IoT.

The TPMin problem is formulated as

$$\begin{aligned}
\mathbf{P}: \underset{\mathbf{w},p_t}{\text{minimize}} \;\; & p_t, && \text{(8a)}\\
\text{subject to} \;\; & C_1: R_k \geq R_k^{\text{th}}, \quad \text{for} \quad k \in \mathcal{K}_0, && \text{(8b)}\\
& C_2: \eta_b(1-\alpha)|\mathbf{h}_k^{\text{H}}\mathbf{w}|^2 p_t \geq p_b, \;\text{for}\; k \in \mathcal{K}, && \text{(8c)}\\
& C_3: \|\mathbf{w}\|^2 = 1, && \text{(8d)}\\
& C_4: |\mathbf{g}_1^{\text{H}}\mathbf{w}|^2 \geq \ldots \geq |\mathbf{g}_K^{\text{H}}\mathbf{w}|^2. && \text{(8e)}
\end{aligned}$$

The problem, $\mathbf{P}$, is non-convex since the constraints of $\mathbf{P}$ are not convex functions in either of the optimization variables, i.e., $\mathbf{w}$ and $p_t$, and are thus difficult to solve optimally. As a result, we first convert the problem to convex form and use SDR techniques to find the sub-optimal solution for $\mathbf{P}$. Next, we propose and develop solutions to $\mathbf{P}$.

## IV. Proposed Solution

To solve the problem $\mathbf{P}$, we first replace the rate of each tag, given in (4), with its lower bound for mathematical tractability. From (4) the lower bound is derived as

$$\begin{aligned}
\mathcal{R}_k \;&=\; \mathbb{E}_x\left\{\log_2\left(\frac{1+(a_k+b_k)x(n)}{b_k x(n)+1}\right)\right\}\\
&\geq \underbrace{\mathbb{E}_x\left\{\log_2\left(1+(a_k+b_k)x(n)\right)\right\}}_{\text{Lower bound}}\\
&\quad - \underbrace{\mathbb{E}_x\left\{\log_2\left(1+b_k x(n)\right)\right\}}_{\text{Upper bound}}\\
&\overset{(a)}{=} \log_2\left(1+\frac{(a_k-b_k)}{2(1+b_k)}\right) \triangleq \mathcal{R}_k^{\text{lb}}, \qquad \text{(9)}
\end{aligned}$$

where $a_k$ and $b_k$ are given in (7), and $x(n) = |s(n)|^2$. In (9), the step $(a)$ is obtained by using $\mathcal{F}_{\text{lb}} \leq \mathbb{E}_x\{\log_2(1+f(x))\} \leq \mathcal{F}_{\text{ub}}$ [14], where $\mathcal{F}_{\text{ub}} = \log_2(1+\mathbb{E}_x\{f(x)\})$, and $\mathcal{F}_{\text{lb}} = \log_2(1+[\mathbb{E}_x\{1/f(x)\}]^{-1})$, in which $\mathbb{E}_x\{1/f(x)\} = 1/\mathbb{E}_x\{f(x)\} + \sigma^2_{f(x)}/[\mathbb{E}_x\{f(x)\}]^3$.

We next convert the rate requirement constraints in (8b) to SINR constraints and reformulate $\mathbf{P}$ as

$$\begin{aligned}
\mathbf{P}_{\text{p}}: \underset{\mathbf{w},p_t}{\text{minimize}} \;\; & p_t, && \text{(10a)}\\
\text{subject to} \;\; & C_1': \gamma_k \geq \gamma_k^{\text{th}}, \quad \text{for} \quad k \in \mathcal{K}_0, && \text{(10b)}\\
& C_2 - C_4. && \text{(10c)}
\end{aligned}$$

Problem $\mathbf{P}_{\text{p}}$ is a non-convex since the constraints are non-convex with respect to $\mathbf{w}$. Further, this quadratic problem is NP-hard, making it challenging to solve in its current form [15]. We thus utilize the SDR technique to solve $\mathbf{P}_{\text{p}}$.

The SDR of a problem is achieved by relaxing some of its constraints and expanding the domain of the objective function [16]. Therefore, all possible solutions of $\mathbf{P}_{\text{p}}$ are feasible for the SDR, and the optimal SDR value represents an upper bound on the optimal value of $\mathbf{P}_{\text{p}}$ [16]. We specifically relax the non-convex rank one constraint, which is the only challenging constraint to deal with when using semi-definite programming (SDP) and use SDP to solve the relaxed problem.

To this end, we first define $\mathbf{v} \triangleq \sqrt{p_t}\mathbf{w}$, $\mathbf{W} \triangleq \mathbf{v}\mathbf{v}^{\text{H}}$, and $\mathbf{A} \triangleq \mathbf{a}\mathbf{a}^{\text{H}}$, where $\mathbf{a} \in \{\mathbf{f}, \mathbf{g}_k, \mathbf{h}_k\}, k \in \mathcal{K}$, and rewrite the SINR terms in (3) as

$$\gamma_0 = \frac{\text{Tr}(\mathbf{F}\mathbf{W})}{\alpha\sum_{i\in\mathcal{K}}\text{Tr}(\mathbf{G}_i\mathbf{W})+\sigma^2}, \qquad \text{(11)}$$

and (5) as

$$\gamma_k = \frac{\alpha\,\text{Tr}(\mathbf{G}_k\mathbf{W}) - \alpha\sum_{i\in\mathcal{K}_k'}\text{Tr}(\mathbf{G}_i\mathbf{W})}{2\left(\alpha\sum_{i\in\mathcal{K}_k'}\text{Tr}(\mathbf{G}_i\mathbf{W})+\sigma^2\right)}. \qquad \text{(12)}$$

Thereby, $\mathbf{P}_{\text{p}}$ is equivalently reformulated as

$$\begin{aligned}
\mathbf{P}_{\text{p1}}: \underset{\mathbf{W}}{\text{minimize}} \;\; & \text{Tr}(\mathbf{W}), && \text{(13a)}\\
\text{subject to} \;\; & C_1': \gamma_k \geq \gamma_k^{\text{th}}, \quad \text{for} \quad k \in \mathcal{K}_0, && \text{(13b)}\\
& C_2': \eta_b(1-\alpha)\,\text{Tr}(\mathbf{H}_k\mathbf{W}) \geq p_b, && \text{(13c)}\\
& C_3': \text{Tr}(\mathbf{W}) \leq p_{\max}, && \text{(13d)}\\
& C_4': \text{Tr}(\mathbf{G}_1\mathbf{W}) \geq \ldots \geq \text{Tr}(\mathbf{G}_K\mathbf{W}), && \text{(13e)}\\
& C_5: \text{Rank}(\mathbf{W}) = 1, && \text{(13f)}
\end{aligned}$$

where $p_{max}$ is the maximum allowable transmit power at the BS. Since the rank-one constraint in (13f) is highly non-convex, relaxing it allows $\mathbf{P}_{\text{p1}}$ to be reformulated as the following SDR problem [4], [15]:

$$\begin{aligned}
\mathbf{P}_{\text{p2}}: \underset{\mathbf{W}}{\text{minimize}} \;\; & \text{Tr}(\mathbf{W}), && \text{(14a)}\\
\text{subject to} \;\; & C_1' - C_4'. && \text{(14b)}
\end{aligned}$$

Here, $\mathbf{P}_{\text{p2}}$ is the SDR of $\mathbf{P}_{\text{p1}}$, which is an SDP problem. Furthermore, $\mathbf{P}_{\text{p2}}$ is a convex optimization problem that can be solved with SDP in CVX Matlab [15], [17]. If the solution to the relaxed-SDR problem, $\mathbf{P}_{\text{p2}}$, is of rank one, i.e., $\mathbf{W}^o = \mathbf{v}^o(\mathbf{v}^o)^{\text{H}}$, the optimal solution to $\mathbf{P}_{\text{p1}}$ is $p_t^o = \text{Tr}(\mathbf{S})$ and $\mathbf{w}^o = \mathbf{v}^o/\sqrt{p_t^o}$, where $\mathbf{S}$ is obtained by evaluating the singular value decomposition (SVD) of $\mathbf{W}^o$ as $\mathbf{W}^o = \mathbf{U}\mathbf{S}\mathbf{U}^{\text{H}}$. Otherwise, we use the Gaussian randomization-based technique to generate an approximated sub-optimal solution to $\mathbf{P}_{\text{p1}}$ to account for the relaxed rank-one constraint [18]. Algorithm 1 summarizes the steps required to solve $\mathbf{P}_{\text{p1}}$.

**Remark 1.** *First, the proposed TPMin problem is converted into a non-convex rank-one SDR problem. After relaxing this rank-one constraint, we solve the relaxed-SDR problem with SDP and then impose the relaxed rank-one constraint with the Gaussian randomization technique. We first set* $\mathbf{w}$ *to feasible values, and then use the steps in Algorithm 1 to update better solutions for* $p_t$ *and* $\mathbf{w}$*. The procedure is repeated until no further progress is made, at which point it is subjected to*

*a termination criterion in which the normalized objective function increment is less than* $\epsilon = 10^{-3}$.

**Algorithm 1** : TPMin ($\mathbf{P}$) - Power/Precoder minimization.

**Initialization**: Begin - CVX.
**Step 1**: Solve the convex problem $\mathbf{P}_{\mathrm{p2}}$ in (14).
**Step 2**: SVD $\mathbf{W}^o$ as $\mathbf{W}^o = \mathbf{U}\mathbf{S}\mathbf{U}^{\mathrm{H}}$, where $\mathbf{U} = [\mathbf{u}_1, \ldots, \mathbf{u}_M]$.
End - CVX.
**if** $\mathrm{Rank}(\mathbf{W}^o) = 1$, **then**
**return**: $p_t^o = \mathrm{Tr}(\mathbf{S})$ and $\mathbf{w}^o = \mathbf{u}_1$.
**else**
**for** $d = 1, \ldots, D$ **do**
1: Generate random $\mathbf{v}_d = \mathbf{U}\mathbf{S}^{1/2}\mathbf{e}_d$, where $\mathbf{e}_d = [\mathrm{e}^{j\phi_1}, \mathrm{e}^{j\phi_2}, \ldots, \mathrm{e}^{j\phi_M}]^{\mathrm{H}}$ and $\phi_i \sim \mathcal{U}(0, 2\pi)$.
2: Check if $\mathbf{P}_{\mathrm{p2}}$ is feasible with $\mathbf{v}_d$.
**end for**
**return**: $p_t^o = \|\mathbf{v}^o\|^2$ and $\mathbf{w}^o = \mathbf{v}^o/\sqrt{p_t^o}$, where $\mathbf{v}^o = \arg\min_{d=1,\ldots,D} \mathbf{v}_d$.
**end if**

**Output:** Optimal transmit power $p_t^o$ and precoder $\mathbf{w}^o$.

**TABLE I:** Simulation settings.

| Parameter | Value | Parameter | Value |
|---|---|---|---|
| Bandwidth | 10 MHz | $d_f$ | 12 m |
| Noise figure | 10 dB | $d_{h_1}, d_{h_2}$ | 4 m, 5 m |
| $p_b$ | $-20$ dBm | $d_{q_1}, d_{q_2}$ | 10 m |
| $\eta_b$ | 0.6 | $M$ | 32 |

### A. Computational Complexity

The SDR problem in $\mathbf{P}_{\mathrm{p2}}$ is traditional SDP, and it is solved with well-known interior point techniques [19]. For Algorithm 1, given the number of constraints, the interior point techniques with a matrix $\mathbf{W}$ with variables of size $M \times M$ will need $\mathcal{O}(\sqrt{M}\log(1/\kappa))$ iterations, with each iteration requiring $\mathcal{O}(M^6)$ arithmetic operations in the worst case, where $\kappa$ is the accuracy of the interior-point method [4], [19].

## V. Simulation Results

Herein, we present simulation results for evaluating the performance of the NOMA-enabled BackCom system. We use the 3GPP urban micro (UMi) model model the large-scale fading, $\zeta_{\mathbf{a}}$, with $f_c = 3$ GHz operating frequency [20, Table B.1.2.1]. Furthermore, we model the AWGN variance, $\sigma^2$, as $\sigma^2 = 10\log_{10}(N_0 B N_f)$ dBm, where $N_0 = -174$ dBm/Hz, $B$ is the bandwidth, and $N_f$ is the noise figure. The simulation parameters are summarized in Table I.

To evaluate the performance of the SR network and characterize the advantages of NOMA, we consider two different scenarios including one benchmark and the proposed system as follows:

- $C_1$ *SR - OMA*: A setup with only one user and one tag. The user decodes its data first, and then uses SIC to decode the tag signal.
- $C_2$ *SR - NOMA*: The proposed system setup consists of a single user and multiple tags. The proposed NOMA beamforming scheme is used to serve the tags.

To compare the performance of the optimal beamforming design, we consider *random beamforming* at BS as a benchmark, i.e., a randomly generated normalized vector is selected such that constraint (8e) is satisfied. The rate requirements for the user, $T_1$, and $T_2$ are set to $\mathcal{R}_0^{\mathrm{th}} = 4$ bps/Hz, $\mathcal{R}_1^{\mathrm{th}} = 2\mathcal{R}_{\mathrm{th}}$, and $\mathcal{R}_2^{\mathrm{th}} = \mathcal{R}_{\mathrm{th}}$, respectively, where $\mathcal{R}_{\mathrm{th}}$ is the lowest rate requirement of a tag, i.e., the minimum tag rate threshold.

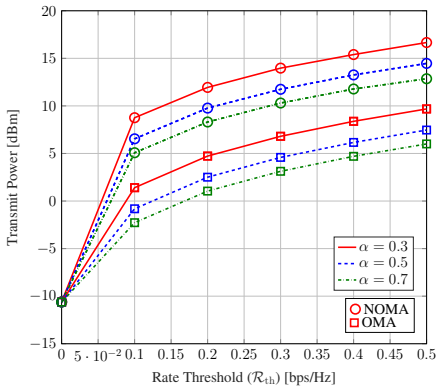


**Fig. 2:** The minimum transmit power as a function of rate threshold ($\mathcal{R}_{\mathrm{th}}$).

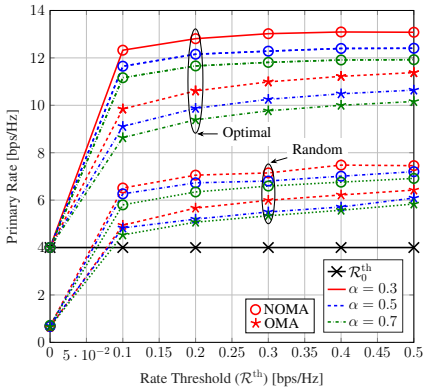


**Fig. 3:** Primary user rate as a function of rate threshold ($\mathcal{R}_{\mathrm{th}}$).

Fig. 2 shows the minimum transmit power as a function of $\mathcal{R}_{\mathrm{th}}$ for various tag reflection coefficients, $\alpha$. When the tags require zero rates, i.e., when the tag does not exist, the purpose is to maintain the user's rate. Hence, in both OMA and NOMA cases, the BS transmits at $-10$ dBm transmit power (Fig. 2) while satisfying the user's minimum rate requirement (Fig. 3). Nevertheless, as the tags demand non-zero rate requirements, i.e., when $\mathcal{R}_{\mathrm{th}}$ increases, the BS has to allocate more power to satisfy the rates of the user and the tags simultaneously. For example, the proposed NOMA scheme with $\alpha = 0.5$ causes a transmit power of 11.7 dBm to achieve the minimum rates of 0.3 bps/Hz and 0.6 bps/Hz for $T_1$ and $T_2$, respectively, while maintaining the user's rate and tags' EH requirements. This power demand increases by 2.8 dBm when the minimum tag rates for $T_1$ and $T_2$ rise to 0.5 bps/Hz and 1 bps/Hz, respectively. Compared to OMA with only $T_1$, the proposed NOMA approach needs $\sim$7 dBm more power to meet the minimum rate requirements of tags regardless of $\alpha$. With this additional power, however, the proposed NOMA system can achieve a higher rate for the user (Fig. 3) while maintaining the rates of both tags (Fig. 4). Additionally, as $\alpha$ decreases, transmit power increases for specific tag rate requirements. This is because the tags reflect less power and harvest more.

Fig. 3 and Fig. 4 plot the user rate and tag rates as a function

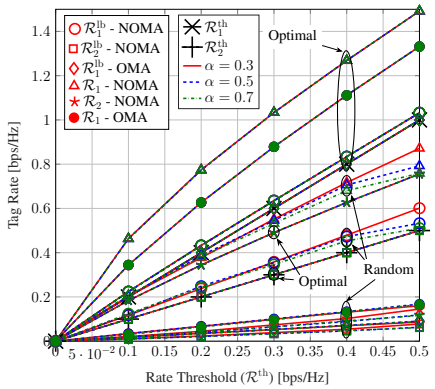


**Fig. 4:** Tag rates as a function of rate threshold ($\mathcal{R}_{\text{th}}$).

of $\mathcal{R}_{\text{th}}$. To evaluate the performance of our proposed method, we also investigate the achieved rates of the devices when the BS adopts random beamforming. However, it cannot satisfy the user and tag rate requirements, so SR is not feasible. On the other hand, our beamforming design can maintain those requirements and further improve the performance. Therefore, our algorithm enables green SR under low transmit powers.

In Fig. 3, when the tags require zero rates, the goal is only to maintain the user's rate. The user reaches higher rates than the respective threshold rates when $\mathcal{R}_{\text{th}}$ grows. Since the BS allocates more transmit power to maintain the rates of tags, the rate improvement of the user of the proposed NOMA scheme is more significant than that of the OMA. For instance, for $\mathcal{R}_{\text{th}} = 0.3\,\text{bps/Hz}$ and $\alpha = 0.5$, this rate improvement is $2\,\text{bps/Hz}$, whereas the user of the proposed scheme achieves an $8\,\text{bps/Hz}$ higher rate than the respective threshold rate, $\mathcal{R}_0^{\text{th}} = 4\,\text{bps/Hz}$. As per Fig. 3, our proposed TPMin approach ensures the user's rate requirement regardless of $\alpha$. The user achieves higher rates for low $\alpha$ values than for high $\alpha$ values, owing to higher transmit power being assigned at the BS for low $\alpha$ values (Fig. 2).

Fig. 4 illustrates the tag's actual (6) and lower bound (9) rates. It shows that the tight rate lower bound adopted for the proposed TPMin problem satisfied the minimum rate requirements of the tags for different values of $\alpha$, whereas the actual rate of the tag is always greater than the required rate. Specifically, since $T_2$ has the worst channel gain in the proposed NOMA scheme, its lower bound matches the required rate, while $T_1$'s lower bound is slightly higher. This is because the tag with the lowest channel gain, i.e., $T_2$, requires more power to maintain rete. When the lowest tag's rate is satisfied, the primary user and the rest of the tags, i.e., with higher channel gains, achieve higher rates than their threshold.

## VI. Conclusion

This paper investigated an SR system with a primary cellular user and NOMA-enabled backscatter tags. We designed an optimal BS beamformer to simultaneously serve the primary user and NOMA-enabled backscatter tags. The beamforming vector minimizes the BS's transmit power while maintaining the minimum rate requirements of the user and the tags, and the EH requirements of the tags. Because this resource allocation problem is non-convex, we used the SDR technique to solve it. We can guarantee the QoS of both the primary user and the tags, enabling multiple access in backscatter systems with no modifications or additional processing at the tag. Hence, the cost and size benefits of passive tags are preserved in our setup, enabling the potential development of ambient IoT solutions.

## References


[1] "3GPP TSG RAN −97e3, Study on ambient IoT , 9.1 (from RP-222685)," Sep. 2022. Available Online: https://portal.3gpp.org/ngppapp/TdocList.aspx?meetingId=60043.

[2] D. Galappaththige, F. Rezaei, C. Tellambura, and S. Herath, "Link budget analysis for backscatter-based passive IoT," *IEEE Access*, vol. 10, pp. 128 890–128 922, Dec. 2022.

[3] F. Rezaei, D. Galappaththige, C. Tellambura, and S. Herath, "Coding techniques for backscatter communications - A contemporary survey," *IEEE Commun. Surveys Tuts.*, pp. 1020–1058, 2th Quart. 2023.

[4] R. Long, Y.-C. Liang, H. Guo, G. Yang, and R. Zhang, "Symbiotic radio: A new communication paradigm for passive internet of things," *IEEE Internet Things J.*, vol. 7, no. 2, pp. 1350–1363, Feb. 2020.

[5] D. T. Hoang, D. Niyato, D. I. Kim, N. V. Huynh, and S. Gong, *Ambient Backscatter Communication Networks*. Cambridge University Press, 2020.

[6] G. Wang, F. Gao, R. Fan, and C. Tellambura, "Ambient backscatter communication systems: Detection and performance analysis," *IEEE Trans. Wireless Commun.*, vol. 64, no. 11, pp. 4836–4846, Nov. 2016.

[7] X. Chen, H. V. Cheng, K. Shen, A. Liu, and M.-J. Zhao, "Stochastic transceiver optimization in multi-tags symbiotic radio systems," *IEEE Internet Things J.*, vol. 7, no. 9, pp. 9144–9157, Sep. 2020.

[8] R. Zhang, X. Kang, and Y.-C. Liang, "Minimum throughput maximization for peer-assisted NOMA-plus-TDMA symbiotic radio networks," *IEEE Wireless Commun. Lett.*, vol. 10, no. 9, pp. 1847–1851, Sep. 2021.

[9] Z. Ding, X. Lei, G. K. Karagiannidis, R. Schober, J. Yuan, and V. K. Bhargava, "A survey on non-orthogonal multiple access for 5G networks: Research challenges and future trends," *IEEE J. Sel. Areas Commun.*, vol. 35, no. 10, pp. 2181–2195, Oct. 2017.

[10] M. Shirvanimoghaddam, M. Dohler, and S. J. Johnson, "Massive non-orthogonal multiple access for cellular IoT: Potentials and limitations," *IEEE Commun. Mag.*, vol. 55, no. 9, pp. 55–61, Sep. 2017.

[11] Y. Liao, G. Yang, and Y.-C. Liang, "Resource allocation in NOMA-enhanced full-duplex symbiotic radio networks," *IEEE Access*, vol. 8, pp. 22 709–22 720, Jan. 2020.

[12] F. Rezaei, D. Galappaththige, C. Tellambura, and A. Maaref, "Time-spread pilot-based channel estimation for backscatter networks," *arXiv preprint arXiv:2305.17248*, 2023.

[13] T. Wu, M. Jiang, Q. Zhang, Q. Li, and J. Qin, "Beamforming design in multiple-input-multiple-output symbiotic radio backscatter systems," *IEEE Commun. Lett.*, vol. 25, no. 6, pp. 1949–1953, June 2021.

[14] Q. Zhang, S. Jin, K.-K. Wong, H. Zhu, and M. Matthaiou, "Power scaling of uplink massive MIMO systems with arbitrary-rank channel means," *IEEE J. Sel. Topics Signal Process.*, vol. 8, no. 5, pp. 966–981, May 2014.

[15] S. Boyd and L. Vandenberghe, *Convex Optimization*. Cambridge University Press, March 2004.

[16] Z.-q. Luo, W.-k. Ma, A. M.-c. So, Y. Ye, and S. Zhang, "Semidefinite relaxation of quadratic optimization problems," *IEEE Signal Process. Mag.*, vol. 27, no. 3, pp. 20–34, May 2010.

[17] M. Grant and S. Boyd, "CVX: Matlab software for disciplined convex programming, version 2.1," http://cvxr.com/cvx, Mar. 2014.

[18] N. Sidiropoulos, T. Davidson, and Z.-Q. Luo, "Transmit beamforming for physical-layer multicasting," *IEEE Trans. Signal Process.*, vol. 54, no. 6, pp. 2239–2251, June 2006.

[19] E. Karipidis, N. D. Sidiropoulos, and Z.-Q. Luo, "Far-field multicast beamforming for uniform linear antenna arrays," *IEEE Trans. Signal Process.*, vol. 55, no. 10, pp. 4916–4927, Oct. 2007.

[20] "3GPP TR 36.814, further advancements for E-UTRA physical layer aspects, V.9.0.0 Rel. 9," Mar. 2010. Available Online: https://portal.3gpp.org/desktopmodules/Specifications/SpecificationDetails.aspx?specificationId=2493.